JOC Article

Synthesis and Optical Properties of Unsymmetrical Conjugated Dendrimers Focally Anchored with Perylenes in Different Geometries

Yongchun Pan,[†] Meng Lu,[†] Zhonghua Peng,*[,†] and Joseph S. Melinger[‡]

Department of Chemistry, University of Missouri-Kansas City, Kansas City, Missouri 64110, and Naval Research Laboratory, Electronics Science and Technology Division, Code 6812, Washington, D.C. 20375

pengz@umkc.edu

Received May 21, 2003

Two sets of light-harvesting monodendrons with unsymmetrical conjugated phenylacetylene branches and perylene cores, one with π-conjugation from the branches to the core and one without, were synthesized and their photophysical properties were studied by steady-state and time-resolved spectroscopic methods. These monodendrons show comparably high fluorescence quantum yields and efficient energy-transfer properties.

Introduction

Conjugated dendrimers have been extensively studied in recent years.[1] Not only have synthetic methodologies been well-developed and a number of conjugated dendrimers been prepared,[1−4] their applications as new molecular electronic and photonic materials have also been explored.[5−8] In particular, conjugated dendrimers have some unique features which make them attractive candidates as new synthetic light-harvesting materials.[4,9−10] For example, the high density of light-absorbing dendritic branches results in high molar extinction coefficients. Further, the convergent surface-to-core branching structure offers the opportunity for fine-tuning of the electronic state of each segment so that an intrinsic energy gradient may be built into the dendritic structure, which serves as the driving force for the directional energy flow from the branches to the core.[9] Such dendrimers have found applications as light-emitting diodes[5] and fluorescence sensors,[6] and in other photonic devices.[7,8]

We have recently reported unsymmetrical conjugated phenylacetylene (PA) monodendrons.[4] The unique branching structure results in broad absorptions and an intrinsic energy gradient toward the core. To evaluate quantitatively the energy-transfer efficiency and kinetics, and to establish structure−property relationship regarding energy transfer and π-conjugation, a perylene unit serving as an energy trap has been attached to the focal point of the monodendrons. Two types of linkages are adopted, one with perylene directly attached to the monodendrons so that there is an extended π-conjugation between the PA dendron and the perylene units, the other with perylene and the PA monodendrons linked by a benzene ring at meta positions, which disrupts the conjugation and thus provides an extra degree of isolation between the monodendron and the perylene trap. Herein, we present the detailed synthesis of such perylene-anchored monodendrons and the comparison of their optical properties.

Results and Discussion

Synthesis of Perylene-Anchored Monodendrons. Chart 1 shows the structures of the unsymmetrical PA monodendrons anchored with perylenes in direct π-conjugation (**G*n*Per**), while Chart 2 shows the structures of compounds with two PA dendrons and one perylene unit linked through the meta positions of a phenyl ring (**2G*n*Per**). The labels (a, a′, b, c, etc.) are for ^{1}H NMR assignments.

* Corresponding author. Phone: 816-235-2288.
[†] University of Missouri-Kansas City.
[‡] Naval Research Laboratory.

(1) (a) Moore, J. S. *Acc. Chem. Res.* **1997**, *30*, 402. (b) Berresheim, A. J.; Müllen, K. *Chem. Rev.* **1999**, *99*, 1747. (c) Miller, T. M.; Neenan, T. X.; Zayas, R.; Bair, H. E. *J. Am. Chem. Soc.* **1992**, *114*, 1018. (d) Grayson, S. M..; Fréchet, J. M. J. *Chem. Rev.* **2001**, *101*, 3819.
(2) (a) Deb, S.; Madux, T. M.; Yu, L. *J. Am. Chem. Soc.* **1997**, *119*, 9079. (b) Meier, H.; Lehmann, M. *Angew. Chem., Int. Ed.* **1998**, *37*, 643.
(3) Xia, C.; Fan, X.; Locklin, J.; Advincula, R. C. *Org. Lett.* **2002**, *4*, 2067.
(4) (a) Peng, Z.; Pan, Y.; Yu, B.; Zhang, J. *J. Am. Chem. Soc.* **2000**, *122* (28), 6619−6623. (b) Pan, Y.; Lu, M.; Peng, Z. *Polym. Mater. Sci. Eng.* **2001**, *84*, 780.
(5) (a) Wang, P. W.; Liu, Y. J.; Devadoss, C.; Bharathi, P.; Moore, J. S. *Adv. Mater.* **1996**, *8*, 237. (b) Halim, M.; Pillow, J. N. G.; Samuel, I. D. W.; Burn, P. L. *Adv. Mater.* **1999**, *11*, 371.
(6) (a) Pugh, V. J.; Hu, Q.-S.; Pu, L. *Angew. Chem., Int. Ed.* **2000**, *39*, 3638. (b) Gong, L.-Z.; Hu, Q.-S.; Pu, L. *J. Org. Chem.* **2001**, *66*, 2358.
(7) Jiang, D. L.; Aida, T. *Nature* **1997**, *388*, 454.
(8) (a) Lu, M.; Pan, Y.; Peng, Z. *Tetrahedron Lett.* **2002**, *43/44*, 7903. (b)Wang, J.; Pan, Y.; Lu, M.; Peng, Z. *J. Org. Chem.* **2002**, *67* (22), 7781.
(9) (a) Devadoss, C.; Bharathi, P.; Moore, J. S. *J. Am. Chem. Soc.* **1996**, *118* (40), 9635−9644. (b) Xu, Z.; Moore, J. S. *Acta Polym.* **1994**, *45*, 83−87. (c) Shortreed, M. R.; Swallen, S. F.; Shi, Z. Y.; Tan, W.; Xu, Z.; Devadoss, C.; Moore, J. S.; Kopelman, R. *J. Phys. Chem. B* **1997**, *101*, 6318.
(10) (a) Weil, T.; Reuther, E.; Müllen, K. *Angew. Chem., Int. Ed.* **2002**, *41*, 1900. (b) Grebel-Koehler, D.; Liu, D.; De Feyter, S.; Enkelmann, V.; Weil, T.; Engels, C.; Samyn, C.; Müllen, K.; De Schryver, F. C. *Macromolecules* **2003**, *36* (3), 578−590.

10.1021/jo0346858 CCC: $25.00
Published on Web 08/02/2003

CHART 1

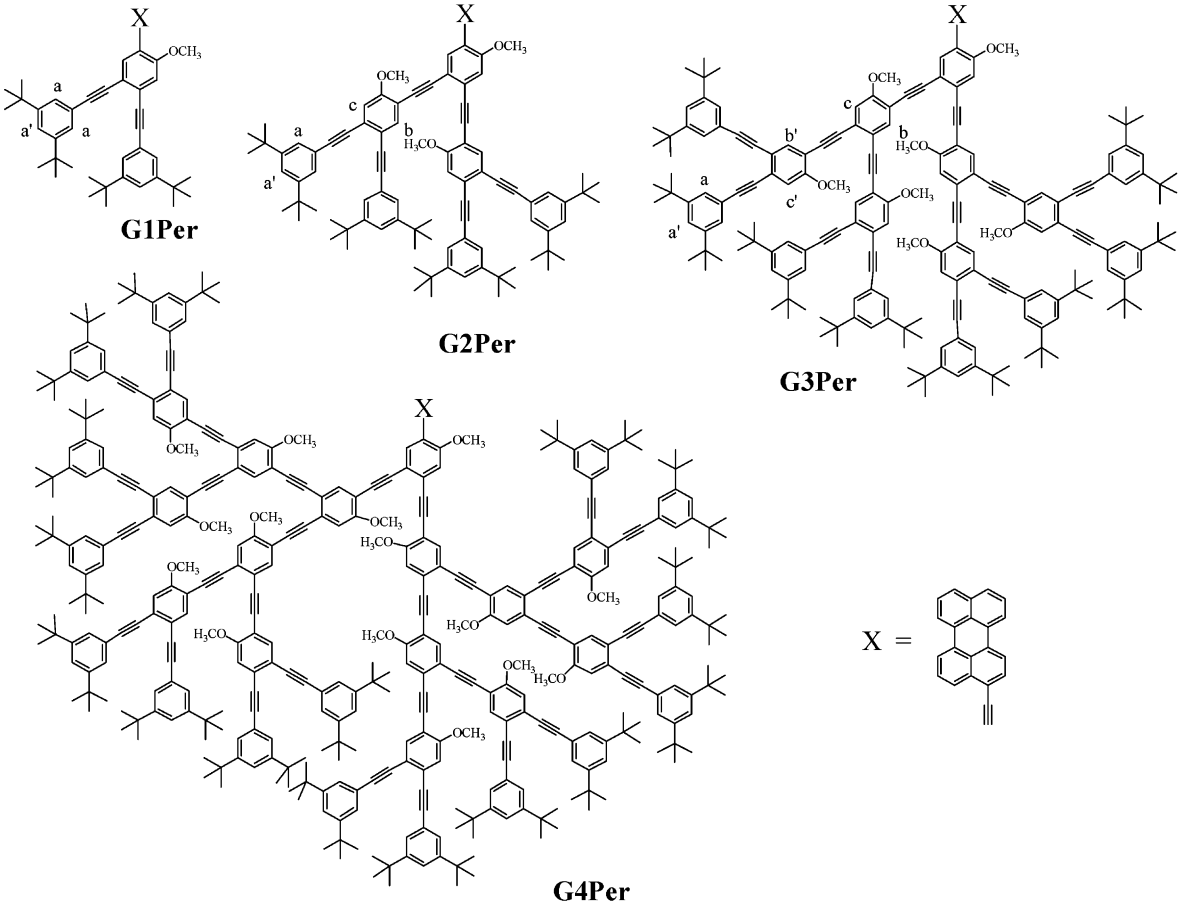

CHART 2

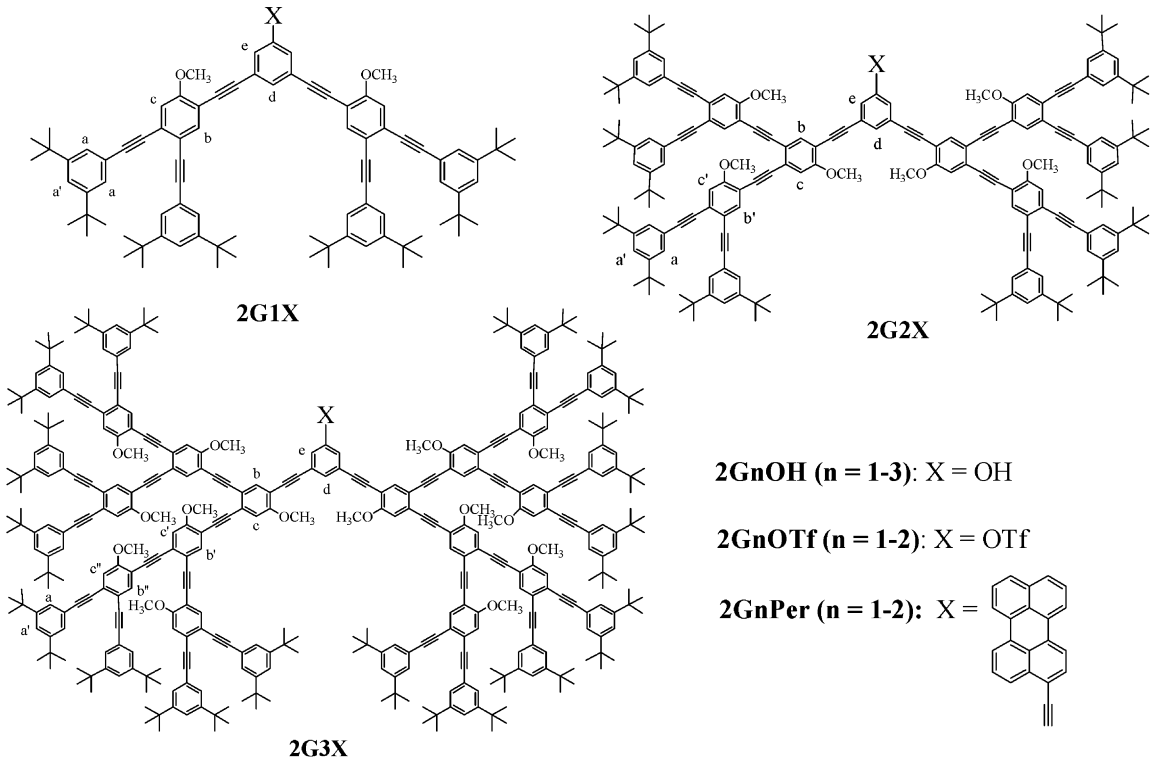

Unsymmetrical PA dendrons with a core phenol group, **G*n*OH** (X = OH in Chart 1), have been reported previously.[4] The phenol group can be readily converted to a triflate (**G*n*OTf**, X = OTf), and from this to an ethynyl

SCHEME 1. Synthesis of Perylene-Terminated Monodendrons

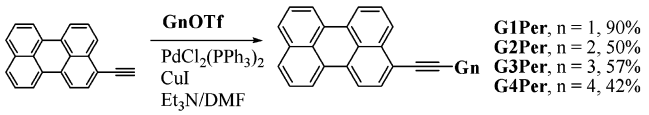

SCHEME 2. Synthesis of 1,3,5-Trisubstituted Benzene Derivatives

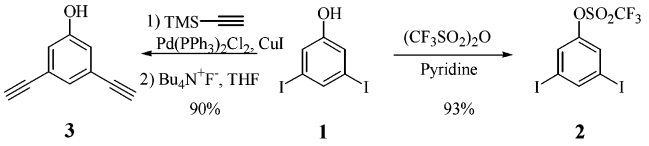

group (**G*n*X**, X = ethynyl) through the Pd-catalyzed Sonogashira coupling reaction. To attach a perylene unit, 3-ethynylperylene was prepared according to a literature procedure.[9a] The coupling reactions of 3-ethynylperylene with triflate-functionalized monodendrons **G*n*OTf** gave the corresponding **G*n*Per** in moderate-to-good yields (Scheme 1). All **G*n*Per** have been purified by column chromatography and characterized by ^{1}H NMR, ^{13}C NMR, elemental analysis, and mass spectrometry (MALDI or EI).

To link dendrons and perylene through the meta positions of a phenyl ring, a 1,3,5-trisubstituted benzene, 3,5-diiodophenol **1**, was prepared according to a literature procedure.[11] This compound can be readily converted to 3,5-diiodophenol triflate **2** and 3,5-diethynylphenol **3**, as shown in Scheme 2. All three of these compounds can serve as the bridge to link two PA dendrons and one perylene unit.

The iterative synthesis of **2G*n*Per** is shown in Scheme 3. The mode of synthesis is convergent. Palladium-catalyzed coupling of 3,5-diiodophenol with ethynyl-functionalized monodendrons **G*n*X** (X = ethynyl in Chart 1) gave **2G*n*OH** in excellent yields. The product, which is significantly more polar than the undesired self-coupling side product **2G*n*A** due to the presence of a hydroxyl group, can be easily separated. The reaction of **2G*n*OH** with trifluoromethanesulfonic anhydride in pyridine afforded **2G*n*OTf** in good yields. It should be noted that **2G*n*OTf** may be synthesized in one step from the coupling of **G*n*X** with compound **2**. While the reaction works, the separation of the desired product **2G*n*OTf** from the byproduct **2G*n*A** is quite challenging and repeated chromatography is required. The perylene unit was finally attached by the reaction of **2G*n*OTf** with 3-ethynylperylene. Both **2G1Per** and **2G2Per** were prepared in moderate yields.

A different approach was used to synthesize **2G3OH** due to the difficulty in preparing and purifying acetylene-terminated G3 compound **G3X**. Thus, the coupling reaction between **G3OTf** and 3,5-diethynylphenol produced **2G3OH** in 39% yield. The low yield was due to the separation difficulty and the low stability of 3,5-diethynylphenol.

The structures of **2G*n*OH** (n = 1−3) and **2G*n*Per** (n = 1, 2) were confirmed by ^{1}H NMR and ^{13}C NMR spectroscopy, elemental analysis, and mass spectroscopy.

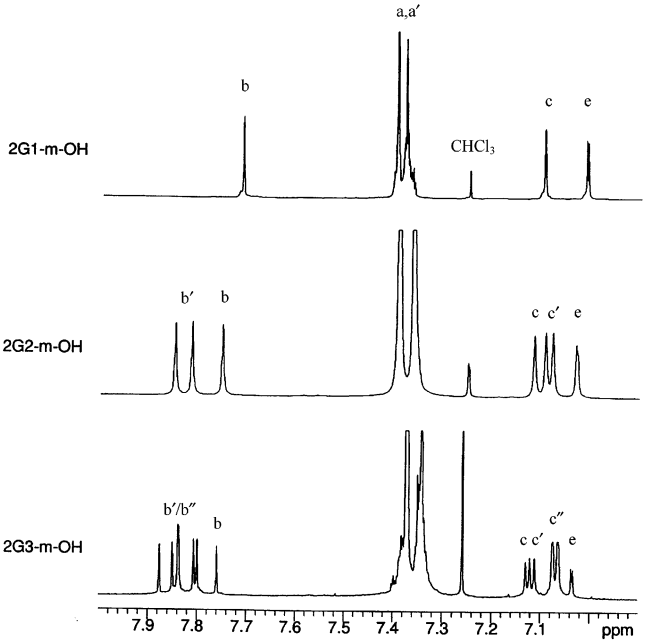

FIGURE 1. Stacked plot of aromatic regions of ^{1}H NMR spectra of **2G*n*OH** in $CDCl_3$ (see Chart 2 for proton labeling).

As shown in Figure 1, the ^{1}H NMR spectra of **2G*n*OH** give well-resolved signals which can be grouped into three regions. The signals with chemical shifts higher than 7.6 ppm are due to the protons ortho to two ethynyl groups in the PA dendron. For **2G1OH** and **2G2OH**, there are one and three singlets, respectively, in this region, consistent with the number of such protons in their respective structure. For **2G3OH**, there are six signals, five of which are singlets and one that is the overlap of two singlets, again consistent with the seven types of such protons in the structure.

The second region of 7.3−7.4 ppm shows two strong and broad signals, which are attributed to the aromatic protons in the peripheral phenyl rings. The proton ortho to two ethynyl groups in the core phenyl rings (proton d in Chart 2) also appears in this region, although it is overlapped with and shadowed by the two strong signals. The third region shows signals with chemical shifts between 7.0 and 7.2 ppm. The well-separated doublet at high field region (7.01 ppm) corresponds to protons ortho to the hydroxy group on the core phenyl ring (proton e in Chart 2). When the size of the dendron increases, this doublet shifts slightly to low fields. Protons ortho to one ethynyl and one methoxy group (protons c/c′/c″) in the PA dendron appear as singlets in this region. The number of peaks is consistent with the types of such protons in their structures. The ^{13}C NMR spectra of **2G*n*OH** provide important structural information as well. The signals in the range of 70−100 ppm correspond to alkynyl carbons. The ^{13}C NMR spectra of **2G1OH** and **2G2OH** show 6 and 14 signals in that range, respectively, consistent with their respective number of alkynyl carbons, while the ^{13}C NMR spectrum of **2G3OH** shows severe signal overlaps.

When perylene is attached to the PA dendron, the ^{1}H NMR spectra become crowded in the aromatic region. However, there are well-separated signals identifiable for both structural units. For example, the ^{1}H NMR spectra of both **2G1Per** and **2G2Per** show five doublets at

(11) Hoeger, S.; Bonrad, K.; Mourran, A.; Beginn, U.; Moeller, M. *J. Am. Chem. Soc.* **2001**, *123* (24), 5651−5659.

SCHEME 3. Synthesis of Meta-Linked Perylene-Anchored PA Dendrons

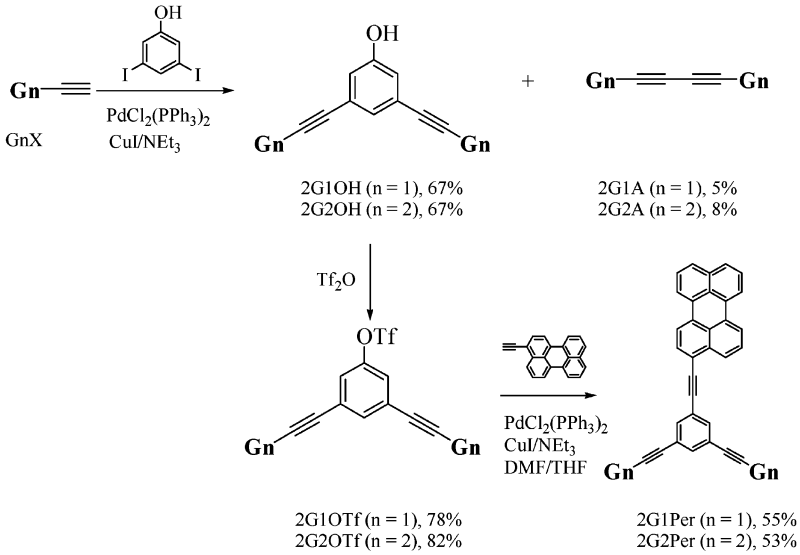

TABLE 1. Optical Properties of Dendritic Compounds

	$\lambda^{ab}{}_{max}{}^{a}$ (nm)	$\lambda^{ab}{}_{edge}{}^{b}$ (nm)	$\epsilon_{max}{}^{c}$ (M^{-1} cm^{-1})	$\lambda^{em}{}_{max}{}^{d}$ (nm)	$\phi_{fl}{}^{e}$	$\phi_{ET}{}^{f}$	t^{g} (ns)
2G1OH	304	394	130 000	399	0.70		1.8
2G2OH	322	430	260 000	432, 454(sh)	0.81		1.9
2G3OH	324	448	500 000	448, 475(sh)	0.71		1.6 (95%),2.6 (5%)
2G1Per	304	490	160 000	485, 517(sh)	0.75	0.96	2.2
2G2Per	308	490	330 000	485, 517(sh)	0.71	0.94	2.2
G1OH	283	356	48 000	360, 374 (sh)	0.40		1.7
G2OH	299	416	82 500	417, 438 (sh)	0.81		2.0
G3OH	310	440	171 000	440, 466 (sh)	0.70		1.9
G4OH	321	453	330 000	452, 479 (sh)	0.65		1.7 (91%), 2.7 (9%)
G1Per	275, 482	500		491	0.74	0.93	2.2
G2Per	298, 485	503		497	0.80	0.85	2.0
G3Per	304, 485	504		498	0.77	0.91	1.9
G4Per	305, 486	504		498	0.74	0.90	1.5 (93%), 2.7 (7%)

[a] Maximum absorption wavelengths. [b] Absorption band edge. [c] Molar extinction coefficients at the absorption maximum. [d] Fluorescence emission wavelengths. [e] Fluorescence quantum yields (ϕ_{fl}). [f] Energy transfer efficiencies. [g] Fluorescence lifetimes.

chemical shifts over 8.2 ppm and two triplets at 7.66 and 7.55 ppm, all of which can be assigned to the aromatic protons in the perylene unit. A high field region between 7.0 and 7.2 ppm corresponds to protons ortho to both the ethynyl and the methoxy groups (protons c/c′) in the PA dendrons. **2G1Per** and **2G2Per** show one and three singlets in this region, respectively. Elemental analysis and mass spectroscopy results support their structures and purity as well.

Optical and Photophysical Properties. The optical properties of **G*n*Per** have been reported previously.[12] This section thus focuses on the properties of **2G*n*OH** and **2G*n*Per**, and the comparison of their optical properties with those of **G*n*OH** and **G*n*Per**, respectively.

The optical properties of all monodendrons, with or without perylene locus, were studied by UV/vis absorption and static-state and time-resolved fluorescence measurements. The photophysical properties of these compounds measured in dichloromethane (DCM) are collected in Table 1.

Figure 2 shows the absorption spectra of the **2G*n*OH** series and **G*n*OH** series. The two sets of monodendrons show some similar features in their absorption behavior. With increasing generation, both sets of dendrons exhibit a broader absorption wavelength range and higher molar extinction coefficients. It is noted that the absorption band edges of **2G*n*OH** are higher than that of **G*n*OH**, but lower than that of **G(*n*+1)OH**. It is reasonable to compare **2G*n*OH** to **G(*n*+1)OH** since they have similar components and molecular size. They differ in the way that smaller monodendrons are connected to the central benzene ring. For **2G*n*OH**, monodendrons **G*n*** are attached at both meta positions to the phenolic hydroxy group, whereas for **G(*n*+1)OH**, monodendrons **G*n*** are linked unsymmetrically at the para and the meta positions relative to the hydroxy group, and thus they are in conjugation at ortho positions relative to each other. Compared to that of the **G*n*OH** monodendron, the extended para conjugated segment of **2G*n*OH** is longer by one phenylacetylene unit, which results in a relative red shift in the absorption band edge. On the other hand, due to the lack of ortho conjugation between the two longest extended conjugation segments, the band edge of **2G*n*OH** is lower than that of **G(*n*+1)OH**. For example, **2G1OH** exhibits an absorption band edge (λ_{edge}) at 394 nm, which is red-shifted by 38 nm from that of **G1OH**, but blue-shifted by 22 nm from that of **G2OH**. Similar results are obtained for higher generation **2G*n*OH**,

(12) Melinger, J. S.; Pan, Y.; Kleiman, V. D.; Peng, Z.; Davis, B. L.; McMorrow, D.; Lu, M. *J. Am. Chem. Soc.* **2002**, *124* (40), 12002−12012.

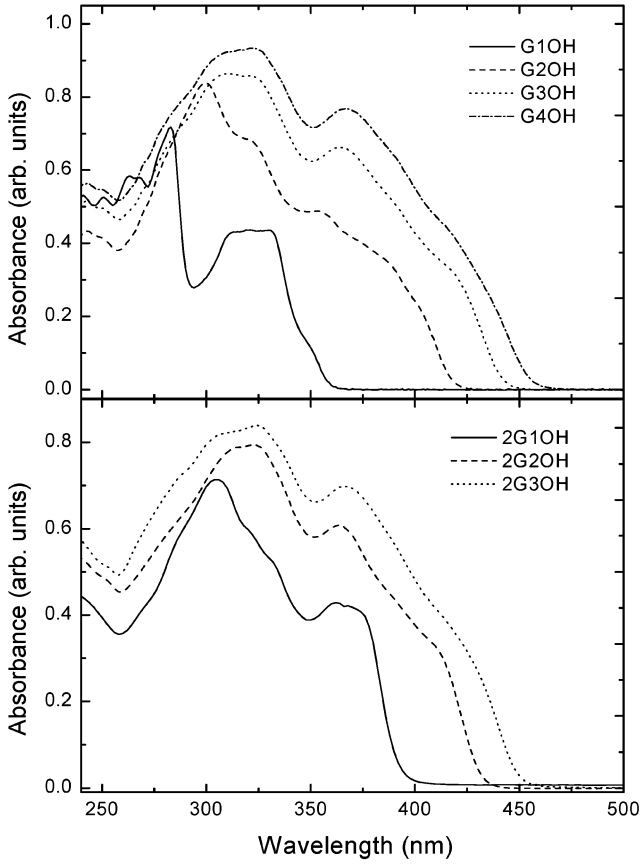

FIGURE 2. UV/vis absorption spectra of **2G*n*OH** and **G*n*OH** in dichloromethane.

though the spectral shift is less significant. **2G3OH** exhibits an absorption band edge at 448 nm, with a 5-nm blue shift from that of **G4OH** and an 8-nm red shift relative to that of **G3OH**. Since **2G3OH** and **G4OH** consist of the same number of phenylacetylene chromophores, the narrower spectral width of **2G3OH** leads to higher absorption intensity at each wavelength, which is reflected by the higher extinction coefficients of **2G*n*OH** over **G(*n*+1)OH** (see Table 1).

The absorption spectra for **2G1Per** and **2G2Per** in DCM are shown in Figure 3. For comparison, the spectra of 3-phenylethynylperylene **4** and **G*n*Per** are also shown in the figure (top). In both sets of perylene-anchored monodendrons, the absorption features of the perylene trap can be clearly distinguished from the PA backbone. It is noted that the absorption band of the perylene trap in **2G*n*Per** is red shifted by just 4 nm from that of compound **4**, in sharp contrast to the nearly 18-nm red shift observed in **G*n*Per**,[12] which indicates that in **2G*n*Per** there are very limited π-electron delocalizations beyond the phenylethynylperylene core, whereas in **G*n*-Per** there are significant electron delocalizations between the perylene and the PA dendrons. The absorption from about 275 to 375 nm is primarily due to the PA backbone since perylene has only weak absorption in this region (see the absorption of **4**). The absorption intensity in this region approximately doubles with each increase in generation.

All PA dendrons are highly fluorescent. As shown in Table 1, the fluorescence quantum yields of **2G*n*OH** and

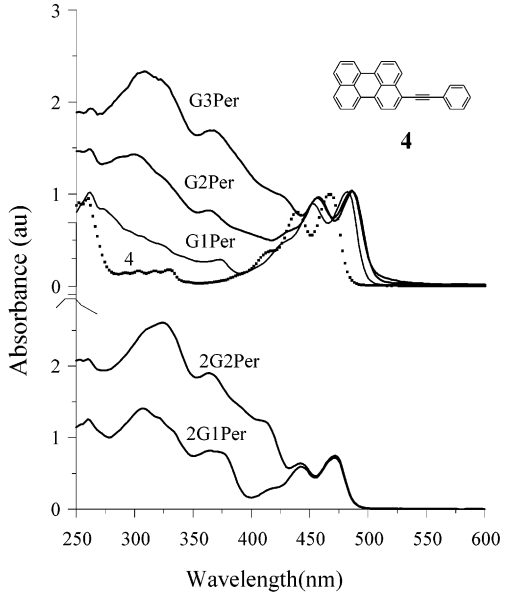

FIGURE 3. Absorption spectra of **2G1Per**, **2G2Per**, **G*n*Per** (n = 1−3), and compound **4** in dichloromethane.

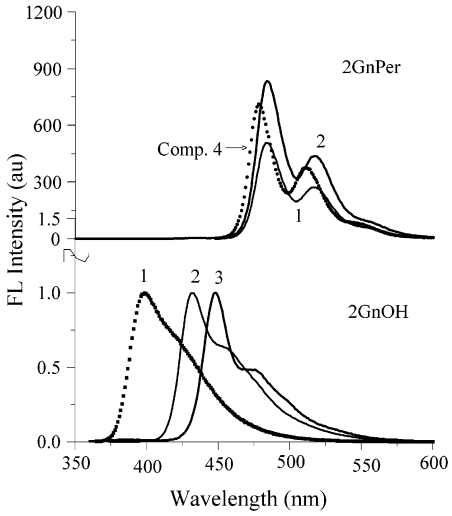

FIGURE 4. Fluorescence emission spectra of **2G*n*OH** and **2G*n*Per** in dichloromethane. The number above each curve represents n.

2G*n*Per monodendrons are in the range of 70−81%, comparable to those of **G*n*OH** and **G*n*Per** monodendrons. The fluorescence dynamics of these monodendrons were measured in DCM, using the technique of time-correlated single-photon counting (TCSPC). The samples were excited with an ca. 1−2 ps laser pulse at 300 nm and the fluorescence decays were monitored at the emission maximum of each of the samples. The fluorescence lifetimes are given in Table 1. The data were analyzed by fitting the transients to a convolution of the instrument response function and a sum of exponential decay functions. As shown in Table 1, the fluorescence lifetimes of **2G*n*OH** are comparable to those of their corresponding **G(*n*+1)OH**, while **2G*n*Per** have slightly longer fluorescence lifetimes than **G*n*Per**. Both **2G1Per** and **2G2Per** have the same lifetime as other perylene-anchored symmetrical PA monodendrons,[9a] which is expected as the fluorescence originates from the same

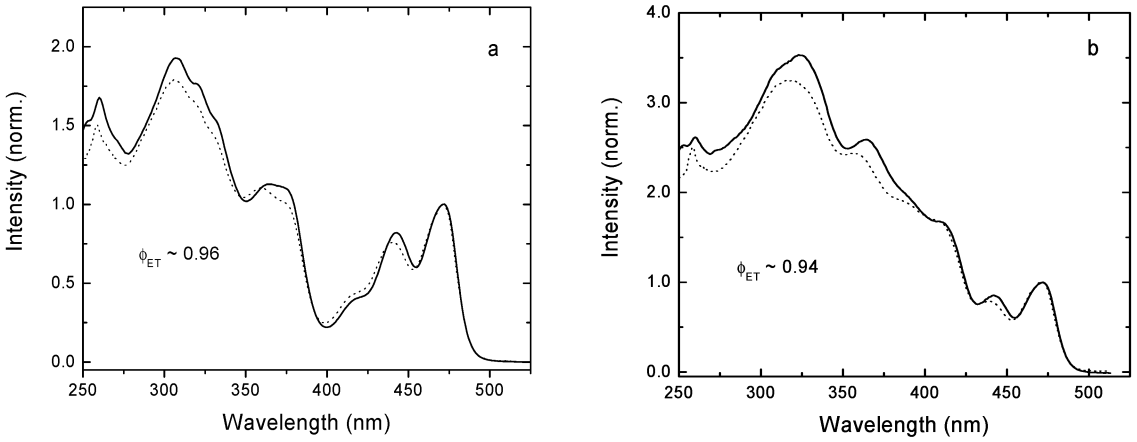

FIGURE 5. Absorption spectrum (solid line) and fluorescence excitation profile (dotted line) normalized to the absorption spectrum in the perylene region: (a) **2G1Per** and (b) **2G2Per**.

phenylethynylperylene core. No obvious correlation is found between the fluorescence quantum yields and fluorescence lifetimes.

The steady-state fluorescence spectra of **2G*n*OH** and **2G*n*Per** in DCM are shown in Figure 4. The emission spectra were obtained by using excitation wavelength at 350 nm. It should be pointed out that the emission maxima and shape of all these monodendrons do not change with variations of excitation wavelengths within their absorption profiles. For the **2G*n*OH** series, the fluorescence spectra are red-shifted with increasing generation. When the perylene unit is attached to the core, however, the emission maximum and shape become independent of the dendron sizes. This is because the emissions from **2G*n*Per** are originated almost entirely from the perylene trap, even though most of the radiation at 350 nm is absorbed by the PA monodendrons, which indicates an efficient energy transfer from the PA dendrons to the perylene trap.

The energy-transfer quantum efficiencies are estimated by comparing absorption and fluorescence excitation profiles (Figure 5). The fluorescence excitation profiles were corrected for the lamp spectrum and the instrumental response, and then normalized by multiplying a factor to best match the absorption spectrum in the perylene region. In each case, the shape and magnitude of the fluorescence excitation profile matches reasonably well with the absorption spectrum. The estimated ET efficiencies fall into the 94−96% range, slightly higher than those of **G*n*Per** monodendrons. In the **2G*n*Per** series, the two unsymmetrical monodendrons are extended away from each other due to meta branching, while in **G*n*Per**, they are crowded together through the ortho linkage. It is possible that the steric crowding of the branches may slightly hinder the energy-transfer process.

Conclusions

A perylene unit as an energy trap has been attached to the unsymmetrical PA dendron in two different geometries, one with π-electron delocalization across the perylene core and the PA branches, the other with localized π-electrons in the perylene trap. The optical properties of **2G*n*OH** and **2G*n*Per** are compared to their corresponding size-equivalent **G(*n*+1)OH** and **G(*n*+1)-Per**. With increasing generations, the absorption band edges and emission wavelengths of **2G*n*OH** shift to the red, a trend observed in the **G*n*OH** series. Compared to **G(*n*+1)OH**, **2G*n*OH** possess a narrower absorption range and shorter fluorescence emission wavelengths, a consequence of the lack of π-electron delocalization between the meta-linked PA dendrons. With perylene attached to the locus, efficient energy transfer from the PA dendrons to the perylene trap is observed for both **2G1Per** and **2G2Per**. Compared to **G(*n*+1)Per**, **2G*n*-Per** exhibit comparable fluorescence quantum yields, slightly longer fluorescence lifetimes, and slightly higher energy-transfer efficiencies. No significant differences in the photophysical properties are found for the two types of perylene-anchored monodendrons. It will be interesting to see how the energy-transfer rates differ in the two sets of perylene-anchored monodendrons. We are currently using the technique of ultrafast pump−probe spectroscopy to explore the excited-state dynamics which shall provide valuable insight into the energy-transfer process.

Experimental Section

The preparations of compounds **G*n*OH** (n = 1−4), **G*n*OTf** (n = 0−4), and **G*n*X** (n = 1−2) were reported previously.[4,13] 3-Ethynylperylene[9a] and 3,5-diiodophenol (**1**)[11] were prepared according to literature procedures.

G1Per. A mixture of **G1OTf** (0.0523 g, 0.0768 mmol), 3-ethynylperylene (0.0267 g, 0.0966 mmol), $Pd(PPh_3)_2Cl_2$ (0.0050 g, 0.00712 mmol), copper(I) iodide (0.0005 g, 0.0026 mmol), triethylamine (0.5 mL), THF (1.0 mL), and DMF (1.0 mL) was stirred at 70 °C for 8 h. The reaction mixture was slowly poured into hydrochloric acid (3 M) and was then extracted with methylene chloride. The organic extracts were washed with water and brine and dried over anhydrous sodium sulfate, and the solvent was then evaporated. The resulting solid was purified by chromatography eluting with hexane/ethyl acetate to yield 0.0555 g of **G1Per** as a red solid (90% yield). ^{1}H NMR (250 MHz, $CDCl_3$, 25 °C, TMS) δ 8.42 (d, J = 8.5 Hz, 1 H), 8.27−8.14 (m, 4 H), 7.83 (s, 1 H), 7.76 (d, J = 8.5 Hz, 1 H), 7.73−7.67 (m, 2 H), 7.61 (t, J = 8.5 Hz, 1 H), 7.55−7.46 (m, 2 H), 7.41−7.39 (m, 6 H), 7.15 (s, 1 H), 4.05 (s, 3 H), 1.28 (s, 36 H); ^{13}C NMR (62.5 MHz, $CDCl_3$) δ 159.4, 151.1,

(13) Pan, Y.; Peng, Z.; Melinger, J. *Tetrahedron* **2003**, *59* (29), 5495−5506.

151.0, 136.6, 134.9, 134.8, 132.6, 131.6, 131.3, 131.2, 131.0, 129.0, 128.7, 128.6, 128.3, 127.6, 127.4, 126.9, 126.8, 126.6, 126.2, 126.1, 123.4, 123.0, 122.5, 122.1, 121.2, 121.0, 120.8, 120.5, 119.9, 119.0, 113.8, 113.4, 96.7, 94.4, 93.9, 91.3, 87.3, 86.3, 56.4, 35.0, 31.5. Anal. Calcd (%) for $C_{61}H_{58}O$ (807.1): C 90.77, H 7.24. Found: C 90.45, H 7.48. MS (MALDI) calcd for $C_{61}H_{58}O$ 807.1, found 806.8.

The synthetic procedure for **G2Per**, **G3Per**, **G4Per, 2G1Per**, and **2G2Per** is similar to that of **G1Per**.

2G1OH. The mixture containing 3,5-diiodophenol (0.130 g, 0.375 mmol), **G1A** (0.442 g, 0.794 mmol), $Pd(PPh_3)_2Cl_2$ (0.0293 g, 0.0423 mmol), and copper(I) iodide (0.0097 g, 0.0509 mmol) and triethylamine (10 mL) was stirred at room temperature for 4 h and was then poured into hydrochloric acid (3 M). The aqueous solution was extracted with CH_2Cl_2. The organic extracts were washed with water and dried over anhydrous sodium sulfate and the solvent was then evaporated. The resulting crude product was purified by flash chromatography with hexane as the eluent to give **2G1OH** as a yellow powder (0.304 g, 67%). ^{1}H NMR (400 MHz, $CDCl_3$) δ 7.72 (s, 2 H), 7.40−7.36 (m, 13 H), 7.10 (s, 2 H), 7.01 (d, J = 1.2 Hz, 2 H), 5.07 (s, 1H), 3.97 (s, 6 H), 1.27 (s, 72 H); ^{13}C NMR (100 MHz, $CDCl_3$) δ 159.3, 155.4, 151.0, 150.9, 137.0, 128.1, 127.6, 126.2, 126.0, 124.9, 123.4, 123.0, 122.5, 122.1, 119.0, 118.8, 113.8, 112.8, 96.7, 94.2, 93.9, 87.2, 86.2, 85.7, 56.3, 35.0, 34.9, 31.5 (two overlapped peaks). Anal. Calcd (%) for $C_{88}H_{98}O_3$ (1203.7): C 87.80, H 8.21. Found: C 87.63, H 8.45. MS (MALDI) calcd for $C_{88}H_{98}O_3$ 1203.7, found 1204.

2G3OH. The synthetic procedure is similar to that of **G1Per**. Yield: 39%. ^{1}H NMR (400 MHz, $CDCl_3$) δ 7.88 (s, 2 H), 7.85 (s, 2 H), 7.84 (s, 4 H), 7.81 (s, 2 H), 7.80 (s, 2 H), 7.76 (s, 2 H), 7.38−7.34 (m, 49 H), 7.13 (s, 2 H), 7.12 (s, 2 H), 7.11 (s, 2 H), 7.08 (s, 4 H), 7.06 (s, 4 H), 7.03 (d, J = 1.2 Hz, 2 H), 5.29 (s, 1 H), 4.00 (s, 6 H), 3.91−3.89 (m, 24 H), 1.26−1.24 (m, 288 H); ^{13}C NMR (100 MHz, $CDCl_3$) δ 159.7, 159.6, 159.6, 159.5 (m) 159.4, 155.5, 151.0 (m), 137.8, 137.5, 137.2, 128.0, 127.9, 127.8, 127.4, 127.3, 127.2, 126.9, 126.1, 126.0, 124.9, 123.3, 122.9, 122.6, 122.6, 122.3, 122.2, 122.2, 119.0, 118.9, 118.6, 118.5 (m), 114.2, 113.9, 113.5 (m), 113.4, 113.3, 113.0, 112.9, 96.8, 96.7, 96.5, 96.4, 94.5, 94.3, 94.2, 94.1, 94.0, 93.9, 93.8, 93.5 (m), 93.3, 91.3, 91.0, 91.0, 88.5, 88.4 (m), 87.4 (m), 87.3 (m), 86.5 (m), 86.3, 85.6, 56.4 (m, four overlapped peaks), 35.0, 34.9, 31.5. Anal. Calcd (%) for $C_{388}H_{410}O_{15}$ (5313.2): C 87.70, H 7.78. Found: C 87.64, H 7.83. MS (MALDI) calcd for $C_{388}H_{410}O_{15}$ 5313.2, found 5312.8.

Acknowledgment. This work is supported by the Office of Naval Research and the Defense Advanced Research Project Agency.

Supporting Information Available: General experimental methods and characterization data (^{1}H and ^{13}C NMR, elemental analysis, and/or mass spectroscopy) for compounds **G*n*Per**, **2G*n*OH**, **2G*n*OTf**, and **2G*n*Per.** This material is available free of charge via the Internet at http://pubs.acs.org.

JO0346858